EAI Endorsed Transactions
on Energy Web
Research Article EAI.EU

Enhancing Power Grid Reliability with AGC and PSO: Insights from the Timimoun Photovoltaic Park

A.A. Tadjeddine[1,2,*], I. Arbaoui[3], R. I. Bendjillali[2], and A. Chaker[1]

[1]SCAMRE Laboratory, Maurice Audin National Polytechnic School of Oran, Algeria
[2]LESTER Laboratory, Department of Electrical Engineering, Nour Bachir University Center, El Bayadh, Algeria
[3]University Ahmed Draia - Adrar, Algeria.

Abstract

This article investigates the impact of integrating Variable Renewable Energy (VRE), specifically solar energy from the Timimoun Photovoltaic Park, on the PIAT electrical grid stability in southern Algeria. The study focuses on how fluctuations in power demand and changes in weather conditions can affect grid frequency control, potentially leading to transient stability issues. To address these challenges, the research proposes the implementation of an Automatic Generation Control (AGC) system combined with the Particle Swarm Optimization (PSO) algorithm to optimize solar energy distribution. This approach effectively regulates real-time frequency deviations resulting from VRE integration, ensuring balanced supply and demand, and controllable power factor injection. The findings demonstrate that the integration of AGC and PSO stabilizes the frequency at the Timimoun Photovoltaic Park and reduces total active losses in the PIAT network by 13.88%. Additionally, strategic power factor control at the injection buses ensures optimal power quality and maximizes the utilization of the photovoltaic park, leading to a 4.84% reduction in the PIAT grid's reliance on gas turbines. This approach contributes to lowering operational costs, reducing carbon emissions, and supporting a transition to greener energy.

Keywords: Renewable Energy Integration, Automatic Generation Control, Particle Swarm Optimization, Electrical Network Stability, Dynamic ZIP loads, Photovoltaic park, PIAT electrical grid.

Received on 02 08 2023, accepted on 20 11 2024, published on 22 11 2024

doi: 10.4108/ew.3669

1. Introduction

The PIAT power infrastructure, which is located in the parched Adrar region of the Algerian desert, presents a significant challenge in terms of effective surveillance and control. Maintaining the integrity of this grid is of the utmost importance, and frequency control has emerged as a primary focus [1, 2].

In a grid with several Distributed Generation Sources (DGS) [3], conventional control approaches have often failed to maintain the frequency needed for a reliable power supply.

One significant challenge is the increasing temperature that is a result of climate change, as evidenced by the fact that temperatures surpassed 50°C in July 2024 [4, 5]. This excessive heat, particularly in isolated regions, exacerbates voltage fluctuations, reduces the stability margin of grid equipment, and intensifies energy consumption [6, 7]. The rise and unpredictability of electrical demand have a direct impact on the dynamic stability of voltage and power factor, as well as the transient stability of grid frequency and active power generation [8, 9].

The integration of Automatic Generation Control (AGC) into multi-zone interconnected power networks has been identified as a viable solution to these concerns. By identifying and rectifying frequency fluctuations, accurate frequency control (AGC) is essential for maintaining a stable system frequency [10]-[14]. This feature is indispensable for the PIAT network, as the primary causes of substantial frequency fluctuations are fluctuations in electrical load and

*Corresponding author. Email: atadj1@gmail.com

the dynamic behaviour of the ZIP load model, particularly in the presence of the frequency coefficient.

The stability of renewable energy systems is further complicated by the sporadic nature of photovoltaic (PV) and wind (WF) energy generation, particularly from the three PV parks in Timimoun (9 MW), Adrar (20 MW), and Kabertene (28.3 MW), as well as the wind farm in Kabertene (10.2 MW). Integrating renewable energy sources, such as the nine MW Timimoun PV Park, which boasts a significant potential of approximately 2,293.7 kWh/m², as illustrated in Fig. 1.

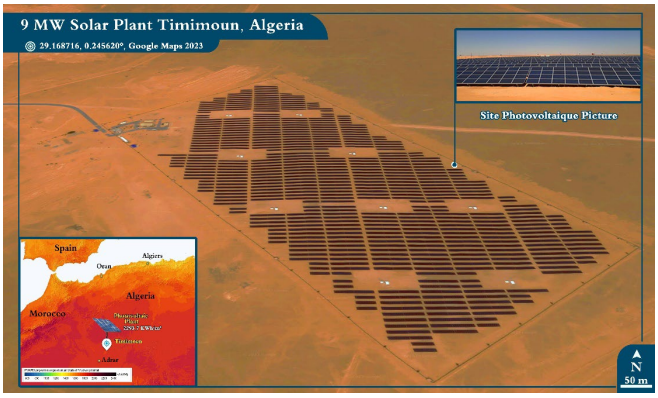

Figure 1. Solar Plant map with average annual power in Timimoun, Algeria

The purpose of this study is to investigate the role of the Automatic Frequency Restoration Reserve (ARRF) in the maintenance of grid frequency by enabling the coordination of Automatic Generation Control (AGC) operations among the gas turbine units situated in Timimoun and Adrar. The 220 kV transmission network and the 60/30 kV distribution system of the PIAT network, which are located in the Adrar province of southern Algeria, are the primary focus of this study. It is essential to comprehend the geographical location of the Timimoun PV Park in order to comprehend the dynamics of the electric grid, as illustrated in Fig. 1, and the single-line diagram of the PIAT network that includes PV generation, as illustrated in Fig. 2.

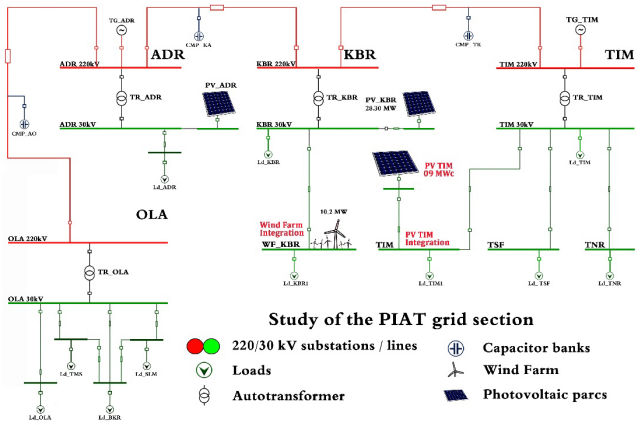

Figure 2. Timimoune photovoltaic injection section study of PIAT electrical grid

The PIAT electrical grid section studied is composed as indicated in Table 1 below:

Table 1. Description of the study system

System characteristics		Number
Buses	Slack bus	1
	PV bus	05
	PQ bus	08
Branches		13
Generators	Gaz Turbine	10
	Wind Farm	01
	PV parcs	03
Autotransformers		08
Shunts		03

This investigation employs small-signal transient stability analysis to examine the mitigation of frequency variations through AGC control, utilising MATLAB 2023b and ETAP 2019. The research also investigates the impact of photovoltaic (PV) integration on the dynamic voltages in the PIAT network, with a particular emphasis on the injection bus at Timimoun. The results emphasise the necessity of meticulous modulation of the injection power factor and local reactive power to maintain operational stability and efficiency.

The equitable distribution of photovoltaic (PV) energy from the Timimoun Park within the network is improved by the utilisation of two power flow analysis algorithms: the Fast Decoupled Load Flow (FDLF) method and the Particle Swarm Optimisation (PSO) method. It is imperative to implement these methods in order to address the challenges associated with the integration of renewable energy sources into the existing grid infrastructure, thereby ensuring both stability and efficiency.

The study of average hourly profiles of photovoltaic (PV) power output reveals that midday hours typically yield the highest PV power output. This corresponds to the time when the sun is at its zenith, providing the most direct and intense sunlight. Consequently, the PV system operates at its peak capacity during these hours, as depicted in Fig. 3.

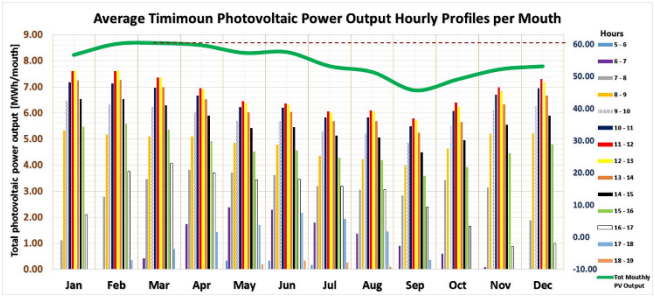

Figure 3. Total Average hourly profiles of photovoltaic output MWh/Mouth

It is crucial to acknowledge that this profile is derived from the assumptions and data used in the study. Actual PV power output profiles can vary based on several factors, such

as location, season, weather conditions, and the specific characteristics of the PV system. These variables affect the amount of sunlight reaching the PV panels, thereby influencing the power output [15].

In addition to frequency control, which is vital for maintaining grid stability [16], reactive power compensation plays a significant role in ensuring overall network stability. Reactive power control is essential for maintaining voltage levels within acceptable ranges, as it balances the reactive power demand and supply within the system. Devices such as capacitors, reactors, and Static Var Compensators (SVCs) actively manage reactive power to regulate voltage levels effectively [17]-[19].

The network frequency is a critical parameter for the nominal operation of the electrical network in Algeria. It has standardised at $f_0 = 50\,Hz$ and has typically maintained within the range of $48 < f < 52\,Hz$. This grid is considered to be in a critical state if any deviation occurs beyond the recommended frequency range [20]. The frequency is generally stable; however, it may be disrupted by fluctuations in power consumption, generator availability, or the adoption of Renewable Energy Sources (RES) [21].

The stability and efficacy of electrical systems are contingent upon the effective control of frequency, which is an essential element of electrical network operation. A precise equilibrium between power supply and demand is required for the efficient operation of energy production, transmission, and consumption [22].

This equilibrium must be systematically monitored to prevent any undesirable deviations from the grid frequency. Device malfunctions, disruptions in power quality, and, in severe cases, potential power failures, can all be significant consequences of frequency fluctuations of this nature [23].

The dynamic regulation of energy generation and consumption in the network architecture is essential for frequency control [24]. A constant frequency that adheres to predetermined constraints is achieved by meticulously designing the intricate control system to precisely balance power production and load demand. The utility grid's overall stability is enhanced by the continuous modification of the power output of generators, which maintains a consistent grid frequency. Consequently, the potential hazards associated with frequency fluctuations are mitigated [25, 26].

The establishment of equilibrium between active energy generation, load consumption, and network losses is a critical objective of frequency regulation. The inertial reaction of synchronous machines promptly restores equilibrium in the event of a disturbance [27]. These machines serve as reservoirs of inertia, which interchange or store kinetic energy with the system to compensate for fluctuations in production and consumption [28].

Consequently, Primary Frequency Control (PFC) is implemented to ensure that the system maintains its dynamic behaviour. The turbine governor (TG) is responsible for regulating the flow rate of the thermodynamic fluid (such as steam, water, or gas) in the turbine that is connected to the synchronous machine's shaft, thereby regulating the amount of active power consumed by synchronous machines through power factor correction (PFC) [20, 27].

By modifying fluid flow to access the inertia reserves of the turbines, power factor correction (PFC) operates swiftly, with a timeframe that can range from a few seconds to tens of seconds. However, Power Factor Correction (PFC) typically minimally affects the power set point of the generators.

By precisely coordinating power facilities within a designated region, secondary frequency control (SFC), also known as AGC, fulfils this function. In comparison to the PFC, the SFC operates at a significantly slower temporal scale, requiring alterations to occur within a range of tens of seconds to minutes. Varieties of time responses for inertia and frequency control are observed in conventional power facilities that employ synchronous machines. These responses can range from 5 seconds for the inertia response of machines to 30 seconds for main frequency control, and up to 20 minutes for secondary frequency control or AGC [29].

The dynamic and essential process of frequency management in electrical systems is contingent upon the efficient coordination and communication among power facilities, transmission systems, and distribution networks. Rapid response and precise control are indispensable for the effective modulation of frequency and the prevention of cascading failures or disruptions that could potentially affect the entire electrical system [23, 25].

Automated Generation Control (AGC) consistently monitors the frequency of the electrical grid, which is essential for this coordination. It transmits control signals to power generators, instructing them to adjust their output, by utilising real-time frequency measurements. The primary objective of Automatic Generation Control (AGC) is to promptly restore the power equilibrium of a system in the aftermath of a disturbance by adjusting the power set points of synchronous machine turbine governors. Consequently, the primary objective of Automatic Frequency Control (AGC) is to accurately monitor the reference frequency, thereby eliminating the frequency inaccuracy that is a result of gas turbine disturbances during periods of stable operation.

As a regional controller, Automatic Frequency Control (AGC) compares a pilot bus or region average frequency to a reference frequency. Due to this comparison, it sends control signals to manage gas turbine production in synchronous equipment [26].

However, because renewable energy production is unpredictable and fluctuating, the increasing integration of renewable energy sources like solar energy into electrical grids presents significant issues for system stability and reliability. Thus, regulatory and control methods must be constantly improved and adjusted. Fig. 4 shows a basic Automatic Generation Control (AGC) system that coordinates n turbogenerators (TGs) in this order:

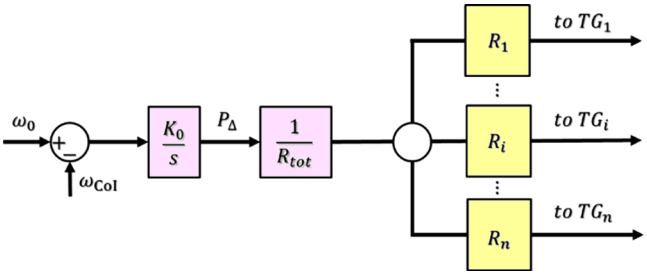

Figure 4. Simplified diagram of an automatic generation control (AGC)

A key controller is incorporated into the AGC system to ensure that the frequency error is zero during steady-state operation. The controller measures the angular frequency of the Centre of Inertia ω_{CoI} and compares it to the reference value of $\omega_0 = 2\pi f_0$.

The control equation undergoes a transformation through the implementation of AGC:

$$\frac{d}{dt}p_\Delta(t) = K_0\left(1 - \omega_{CoI}(t)\right) \quad (1)$$

$$R_{tot} = \sum_{i=1}^{n} R_i \quad (2)$$

Consider the following equation:

$$\hat{P}_{in}(t) = P_G^{ref}(t) + \frac{1}{R}\left(1 - \omega_G(t)\right)\overbrace{+\frac{R}{R_{tot}}p_\Delta(t)}^{\textbf{AGC signal}} \quad (3)$$

Where,

ω_0, equals one in P.u if $f = f_0$, the frequency base.

K_0, integral gain.

R_{tot}, Drops of the turbine governor on P.u (Hz/MW).

R_i, Drop of the turbine governor i.

P_G^{ref}, Power set point of the turbine governor.

P_{in}, is the output of the windup limiter.

$\frac{R}{R_{tot}}p_\Delta(t)$, AGC signals are added to the reference P_G^{ref} of the turbine speed controller.

The inertial response of both the machine and Precision Control (PFC) is comparatively faster than the temporal reaction of Slip-Fooled Control (SFC). The AGC model may be reduced to $p_\Delta(t) = 0$ when conducting fleeting simulations lasting up to 20 or 30 seconds, as the impact of SFC may be insignificant.

$$\hat{P}_{in}(t) = P_G^{ref}(t) + \frac{1}{R}\left(1 - \omega_G(t)\right) \quad (4)$$

AGC systems use the Proportional-Integral-Derivative controller (PID controller) to evaluate the most effective tuning parameters for rapid frequency regulation in order to enhance the precision of primary frequency control and resolve windup issues.

Modifying the scheduled power target to reflect the desired frequency can reduce turbine power extraction during frequency dips. Power plant control systems will adapt more efficiently. Power stations can modify grid frequency and lessen frequency variations by providing a frequency bias. This strategy increases power grid stability and reliability by synchronising power plant activities with the desired frequency and adopting appropriate management measures.

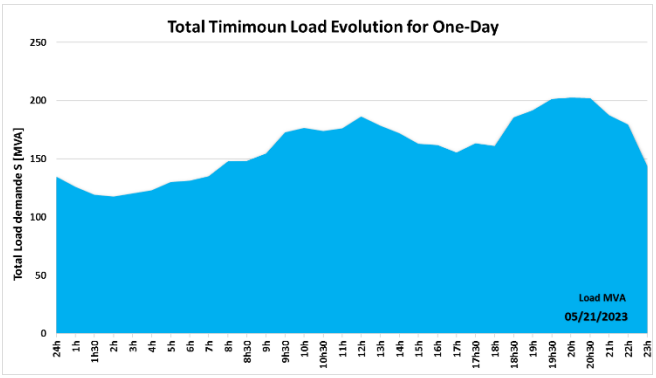

Figure 5. Total loads evolutions in Timimoun substation

In most cases, the relationship between frequency and power grid load is useful for controlling the system, since lowering the frequency usually lowers the overall load. In frequency control investigations, the ZIP model is used to depict the interplay between voltage, active and reactive power, and frequency variations; it captures this dynamic relationship.

$$P_{laod}(f) = P_0(f_{nom}) * \left(1 + m(\Delta f)\right) \quad (5)$$

Where,

m, load-damping factor

When it comes to effective power scheduling and grid stability, the equations of the ZIP model emphasize the significance of voltage levels and frequency sensitivity. Electricity demand peaks at specific times of the day and follows a more regular pattern on weekends, as demonstrated in the daily load profiles, as depicted in Fig. 5.

Figure 6 illustrates the evolution of global partial loads within the PIAT grid during the critical hours between 11:00 AM and 9:00 PM. This timeframe is particularly significant as it captures the period of peak electricity demand. The graph highlights the fluctuations in load demand, reflecting the dynamic nature of electricity consumption throughout the day.

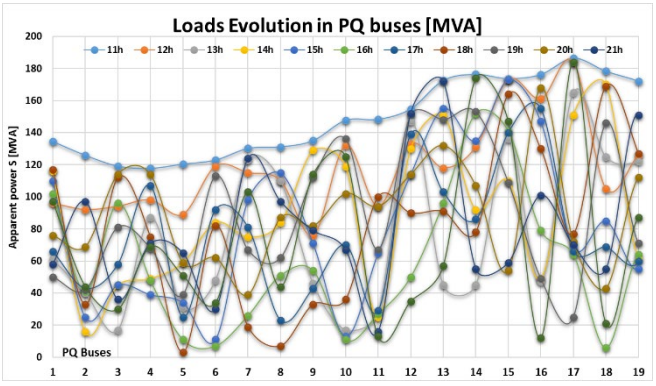

Figure 6. Global partial loads evolutions between 11h-21h

1.1. Related Works

The integration of renewable energy sources (RES) into power grids introduces significant challenges, particularly in terms of frequency stabilization. The inherent variability of RES, such as photovoltaic (PV) and wind farms (WF), necessitates the development and implementation of advanced control mechanisms to ensure grid stability. This section reviews key contributions in this domain, focusing on innovative strategies and methodologies that address these challenges.

Kenyon et al. (2024) introduced the **Droop-e control strategy**, a novel exponential droop control method tailored for grid-forming inverters. This approach addresses frequency stability issues by leveraging a non-linear active power-frequency droop relationship, which enhances the grid's ability to counteract frequency excursions. The Droop-e method significantly reduces the rate of change of frequency (RoCoF) and surpasses traditional linear droop control strategies by incorporating non-linear dynamics, thereby optimizing frequency response under varying load conditions [30].

Chen et al. (2024) provided a comprehensive review of **measurement-based frequency dynamics monitoring** in RES-dominated power systems. The study highlights the critical role of wide area measurement systems (WAMS) in achieving full state awareness and deep informatization of power grids. Chen et al. discuss various data-driven methods for online monitoring of frequency dynamics, emphasizing their potential for more accurate and effective analysis, which is crucial for maintaining grid stability in the face of increasing RES penetration [31].

Dedović et al. (2024) proposed an **adaptive under-frequency load shedding (AUFLS)** scheme that utilizes synchrophasor measurements and Empirical Mode Decomposition (EMD). This innovative approach enhances power system stability during significant disturbances by dynamically adapting to the magnitude of disturbances, frequency response, and voltage stability index. The EMD algorithm, integrated within the AUFLS framework, enables more precise load-shedding decisions, significantly improving system resilience to frequency disturbances [32].

Sahu et al. (2015) developed a **hybrid PSO-PS optimized fuzzy PI controller** for Automatic Generation Control (AGC) in multi-area interconnected power systems. Their approach outperforms conventional and other recently published optimization techniques, demonstrating robustness to wide parameter variations and step load perturbations. The method is also applicable to multi-source, multi-area hydrothermal power systems, with or without High Voltage Direct Current (HVDC) links, further proving its versatility and effectiveness in maintaining frequency stability [33].

Mohapatra et al. (2024) introduced a **type-2 fuzzy tilt control strategy** for AGC in multi-source power grids, optimized using a quasi-opposition pathfinder algorithm (QO-PFA). This novel controller significantly improves frequency stability under various operating conditions and demonstrates superiority over conventional PID controllers. The QO-PFA algorithm also outperforms other optimization techniques, highlighting its potential for broader applications in power system control [34].

Wang et al. (2024) proposed an **optimal AGC allocation strategy** based on data-driven forecasts of key frequency distribution parameters. Utilizing a CNN-LSTM-Attention network, Wang et al. forecast these parameters to optimize AGC allocation coefficients, resulting in improved frequency regulation and reduced costs. Their approach shows marked improvements in minimizing frequency deviations and regulation costs compared to other strategies [35].

Zhao et al. (2024) addressed the challenges of **real-time dispatch** in integrated electric and gas systems (IEGS) with high RES penetration. They developed a multistage stochastic real-time economic dispatch (RTED) model that considers the dynamic interactions between electric power systems (EPS) and natural gas systems (NGS). The decentralized solution effectively mitigates the risk of EPS-side reserve shortages and NGS-side pressure violations, demonstrating its efficacy in managing uncertainty propagation between these interconnected systems [36].

Maucher et al. (2023) explored the **limitations in interzonal exchange** of automatic frequency restoration reserves (aFRR) within Europe. Their study compares different control models for interzonal aFRR exchange under active limitations, providing insights into the impact of transfer capacity limits and finite aFRR availability on system stability [37].

Cremoncini et al. (2024) examined the potential revenue increase from **hybrid battery energy storage systems (HESS)** paired with wind plants. Their model optimizes participation in both day-ahead and aFRR markets, demonstrating significant revenue and system efficiency improvements through battery hybridization [38].

Kang et al. (2024) proposed a distributed, **event-triggered voltage regulation approach** for low-voltage distribution networks (LVDN) with high PV penetration. This method accommodates varying time delays and ensures balanced power sharing among virtual energy storage systems (VESS), thereby improving voltage regulation and system stability [39].

Deman and Boucher (2023) focused on the relationship between **renewable energy generation and power reserve energy demand** in the French power system. Their study addresses a significant gap in the literature, particularly the impact of increasing renewable energy generation on reserve energy demand. They emphasize the importance of understanding this relationship to optimize reserve capacity and maintain grid stability [40].

Tadjeddine et al. (2023) conducted a crucial study on the **integration of Variable Renewable Energy (VRE)** sources into the isolated PIAT grid in Algeria. They addressed the critical issue of maintaining grid stability, particularly voltage and frequency, which are adversely affected by the integration of VRE such as wind and solar power. Their dual approach, involving AFRR for frequency management and local reactive compensation for voltage control, effectively mitigates stability issues, demonstrating significant improvements in network performance and reliability [1].

2. Methods Strategies and Formulation

The Algerian Electrical System Operator (AESO) prioritizes the stability of the PIAT electrical grid, particularly given its integration of renewable energy sources that reduce dependency on natural gas for electricity production. Efficient management of energy distribution from conventional power plants, such as the 182 MWp gas turbines in Adrar and Timimoun, alongside renewable sources like the 38.5 MWp photovoltaic and wind hybrid plant in Kabertene and the 9 MWp and 20 MWp photovoltaic plants in Timimoun and Adrar, is essential for ensuring grid reliability (Fig. 2).

Photovoltaic power plants and wind farms contribute to the grid by generating active power P_{Gi} and reactive power Q_{Gi}, which are injected into the electrical grid. These contributions are vital for maintaining a balanced and stable power supply, while also minimizing costs and environmental impacts.

Our research focuses on balancing power generation (from both gas turbines and renewable sources) with energy consumption (dynamic loads with ZIP characteristics) within the PIAT network. We conduct a comprehensive study on frequency stabilization across all buses in the PIAT network, factoring in the integration of renewable energy sources.

Specifically, we implement an Automatic Generation Control (AGC) system to correct real-time frequency disturbances by regulating the active power output from the Timimoun photovoltaic park, based on electrical consumption and production data from May 21, 2023.

2.1. Automatic Generation Control (AGC)

The step response of frequency deviation, which indicates how the grid's frequency reacts to sudden changes in energy production or load demand, is analyzed in four phases:

1. **Initial Deviation**: The frequency initially deviates from its nominal value when there is a change in electricity production or load demand, depending on the system's responsiveness.
2. **Transient Response**: The frequency enters a phase of adjustment, where it gradually returns towards equilibrium. This phase's duration is influenced by the system's inertia and control mechanisms.
3. **Damping and Recovery**: The frequency deviation is progressively reduced through system controls, such as AGC, which stabilizes the frequency by adjusting active power generation.
4. **Steady State**: Eventually, the frequency stabilizes close to its nominal value, around 50.2 Hz.

The power system model provides real-time feedback on frequency, closing the control loop. This MW Load Frequency Control (LFC) model, equipped with a PI controller, ensures frequency stability by dynamically adjusting generator outputs in response to frequency deviations, maintaining the power system within acceptable limits. Fig. 7 illustrates the block diagram of the closed-loop control system, where the PI controller continuously monitors and processes frequency deviations. The control signal generated by the PI controller is then used to adjust generator set points via the governor control system.

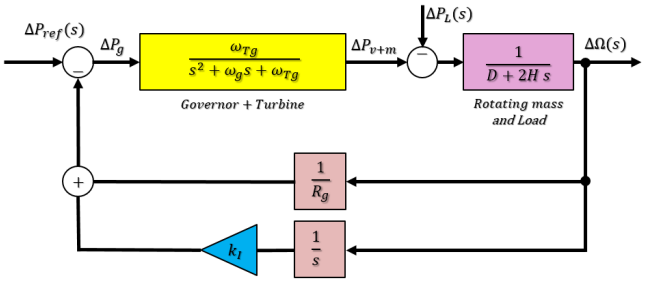

Figure 7. Block diagram model of MW LFC with PI controller

The closed-loop transfer function relating the load change $\Delta \boldsymbol{P_L(s)}$ to the frequency deviation $\Delta \boldsymbol{\Omega(s)}$ is:

$$\frac{\Delta\Omega(s)}{-\Delta P_L(s)} = \boldsymbol{T(s)} = \frac{(1+\tau_g s)(1+\tau_T s)}{(D+2Hs)(1+\tau_g s)(1+\tau_T s)+1/R_g} \quad (6)$$

We have adopted the step input: $\Delta P_L(s) = \Delta P_L/s$

Using the final value theorem, the steady-state value is:

$$\Delta\omega = \lim_{s\to 0} \boldsymbol{s}\,\Delta\boldsymbol{\Omega(s)} = (-\Delta\boldsymbol{P_L})\frac{\boldsymbol{1}}{\boldsymbol{D+1/R_g}} \quad (7)$$

Where: $\boldsymbol{\omega_T}$ represents the turbine pulse frequency, $\boldsymbol{\omega_g}$ denotes the governor pulse frequency, and $\overrightarrow{\boldsymbol{\omega_{Tg}}}$ is the system pulse frequency, defined as the product $\overrightarrow{\boldsymbol{\omega_T}} * \overrightarrow{\boldsymbol{\omega_g}}$. Here, $\boldsymbol{H}$ stands for the generator inertia constant, and $\boldsymbol{R_g}$ refers to the governor speed regulation.

The load varies by 66.82% between 6h and 21h for change in frequency, i.e., D=0.67.

The turbine is designed to generate electricity at a constant frequency of 50Hz, with a rated output of 180 MW in Adrar and Timimoun. However, there is a load change of 67.74 MW($\Delta P_L = 0.376\ per\ unit$) that takes place.

$$\begin{cases} \frac{\Delta\Omega(s)}{-\Delta P_L(s)} = \boldsymbol{T(s)} = \frac{(1+0.2s)(1+0.5s)}{(0.67+10s)(1+0.2s)(1+0.5s)+\frac{1}{0.05}} \\ \boldsymbol{T(s)} = \frac{s^2+7s+10}{50(s^3+7.067s^2+10.469s+20.67)} \end{cases} \quad (8)$$

The steady-state frequency deviation due to a step input is:

$$\begin{cases} \Delta\omega = \lim_{s\to 0}\big(s\,\Delta\Omega(s)\big) = \frac{1}{20.67}(-0.376) \\ \Delta\omega = -0.0182\ p.u \end{cases} \quad (9)$$

Therefore, the application of a 67.74 MW load results in a steady-state frequency deviation of 0.91Hz, which is calculated as $\Delta f = \pm\,|(-0.0182)(50)|$.

For a 20% load change ($(\Delta P_L(s) = 0.2\ \text{p.u})$), with the controller's integral gain set at $k_I = 4$, the closed-loop transfer function that relates the load change to the frequency deviation $\Delta\Omega(s)$ is:

$$\frac{\Delta\Omega(s)}{-\Delta P_L(s)} = T(s) = \frac{s^3+7s^2+10s}{50s^4+353.35s^3+523.45s^2+1033.5s+200} \quad (10)$$

2.2. Generators and loads modelling

The sum of the currents from the loads and the generators connected to the bus_i can present by $\overline{I_i}$:

$$\begin{cases} \overline{I_i} = \sum_{\substack{k=1 \\ k\neq i}}^{N} \overline{Y_{ikp}}\ \overline{V_i} + \sum_{\substack{k=1 \\ k\neq i}}^{N} \overline{Y_{iks}}\ (\overline{V_i} - \overline{V_k}) \\ [I] = [Y]\ [V] \end{cases} \quad (11)$$

Where,

$\overline{Y_{ikp}}$ & $\overline{Y_{iks}}$, parallel and series admittances, respectively.

V_i, Voltage at bus i.

$[I]$, Column vector of order N containing all currents,

$[Y]$, Symmetric matrix of network admittances,

$[V]$, Column vector of order N containing all simple voltages.

Relation 12b can be expressed in a more convenient form by introducing the complex powers S_{Gi} & S_{Li} and eliminating the currents. To achieve this, we define a complex power at bus i as follows:

$$\begin{cases} \overline{S_i} = \overline{V_i}\overline{I_i^*} = P_i + jQ_i \\ \overline{S_i} = (\overline{P_{Gi}} - \overline{P_{Li}}) + j(\overline{Q_{Gi}} - \overline{Q_{Li}}) \end{cases} (12)$$

Where,

I^*, the complex conjugate of I.

P_{sched} and Q_{sched} represent the desired active and reactive powers at an operating voltage V, while P_0 and Q_0 are real powers at the nominal voltage V_0. The coefficients a_p, b_p, c_p, a_q, b_q and c_q determine the relationship between voltage and power outputs in polynomial model. The k_{pf} and k_{qf} parameters indicate the sensitivity to variations in active and reactive powers with respect to voltage variations, typically within specific ranges. Δf Represents the frequency deviation, influencing the dynamic behaviour of the system in response to frequency fluctuations.

In addition, we define:

$$\begin{cases} \overline{V_k} = V_k e^{j\delta_k} \\ \overline{Y_{ik}} = Y_{ik} e^{j\delta_{ik}} \end{cases} \quad (13)$$

Therefore, by combining all these relations, we get:

$$\overline{S_i^*} = \overline{V_i} e^{-j\delta_i} \sum_{k=1}^{n} Y_{ik} e^{j\delta_{ik}} V_k e^{j\delta_k} \quad (14)$$

Where: P_{sched} and Q_{sched} represent the desired active and reactive powers at an operating voltage V, while P_0 and Q_0 are real powers at the nominal voltage V_0. The coefficients a_p, b_p, c_p, a_q, b_q and c_q determine the relationship between voltage and power outputs in polynomial model. The k_{pf} and k_{qf} parameters indicate the sensitivity to variations in active and reactive powers with respect to voltage variations, typically within specific ranges. Δf Represents the frequency deviation, influencing the dynamic conduct of the system in response to frequency fluctuations.

We derived two fundamental equations:

$$\begin{cases} P_i = \sum_{i=0}^{n} (V_i V_K Y_{ik} \cos(\delta_{ik} + \delta_k - \delta_i) \\ Q_i = -\sum_{i=0}^{n} (V_i V_K Y_{ik} \sin(\delta_{ik} + \delta_k - \delta_i) \end{cases} \quad (15)$$

They allow us to relate the active and reactive powers produced (or consumed) at each bus i, to the voltages (in magnitude and phase) present throughout the grid.

$$\begin{cases} P_{sched} = P_0 \left[a_p \left(\frac{V}{V_0}\right)^2 + b_p \left(\frac{V}{V_0}\right) + c_p \right] \left[1 - k_{pf} \Delta f\right] \\ Q_{sched} = Q_0 \left[a_q \left(\frac{V}{V_0}\right)^2 + b_q \left(\frac{V}{V_0}\right) + c_q \right] \left[1 - k_{qf} \Delta f\right] \end{cases} (16)$$

Here, P_{sched} and Q_{sched} represent the desired active and reactive powers at a given operating voltage V, while P_0 and Q_0 denote the corresponding powers at the nominal voltage V_0. The coefficients a_p, b_p, c_p, a_q, b_q and c_q define the relationship between voltage and power outputs in a polynomial model. The parameters k_{pf} and k_{qf} reflect the sensitivity of active and reactive power outputs to voltage variations. Lastly, Δf represents the frequency deviation, affecting the system's dynamic response to frequency fluctuations.

Each bus provides two equations of type 13 & 14, resulting in $2N$ equations. Each bus is also characterized by 6 variables: V_i, δ_i, P_{Gi}, Q_{Gi}, P_{Li}, and Q_{Li}, giving us $6N$ variables initially. To make the system solvable, we need to fix $2N$ unknowns among the $6N$ variables and set $4N$ parameters to known values. The resolution method for this system of equations involves assuming that the dispatcher imposes the network loads; this is the case as long as the grid operates normally. This assumption means fixing the values of P_{Li}& Q_{Li} at each bus i. Therefore, there remain $4N$ variables to be distributed between unknowns and parameters. Up until now, our approach has led us to fix P_{Gi} & P_{Li} at each node of the network. However, this is not realistic because the following relationship must be satisfied:

$$P_l = (\sum_{i=0}^{n} P_{Gi}) - (\sum_{i=0}^{n} P_{Li}) \quad (17)$$

Where: P_l, Total losses in the grid.

These losses cannot be predetermined in the allocation calculation. They are the result of various power flows within the network and cannot be fixed in advance. If we do not know P_l, it is impossible to set all the P_{Gi} & P_{Li} while satisfying equation 17.

The production generators are controlled synchronously with load variations, taking into account all the constraints and limits of the subsystems. The main control lines are summarized in the following Fig. 5. Traditional and effective ways to reduce these problems are to derive additional signals for generator excitation systems and to compensate for fluctuations in power flow through transmission networks.

Figure 8 shows the Flowchart of OPF dynamic ZIP loads with evaluation methods.

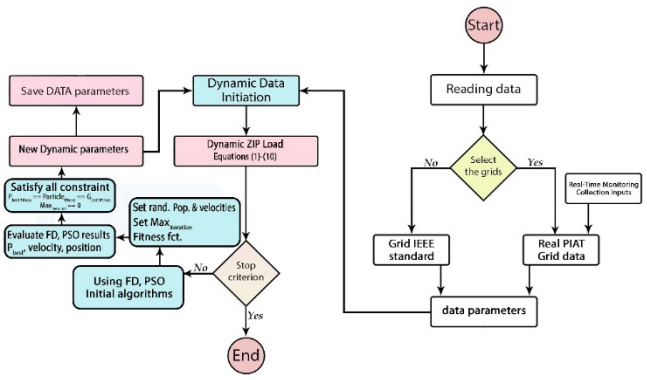

Figure 8. Algorithm flowchart of PSO and D-ZIP loads

3. Results and discussion

The study investigates the role of the Automatic Frequency Restoration Reserve (AFRR) in stabilizing network frequency by coordinating the AGCs of the gas turbine (GTs) units in Timimoun and Adrar. The research examines the PIAT network's 220 kV transmission grid and 60/30 kV distribution system in southern Algeria's Adrar province. Figures illustrate the Timimoun PV Park's location and provide a single-line diagram of the PIAT network with PV outputs. MATLAB 2023b and ETAP 2019 were used for analysis and results representation.

By performing transient stability analysis of small signal disturbances, the AGC controller addresses frequency discrepancies. The study also evaluates the impact of integrating photovoltaic energy on PIAT's dynamic voltages, especially at the Timimoun injection bus. Maintaining the injection power factor or local reactive power within acceptable limits is crucial for managing this integration.

For the Power Flow Analysis (PFA) of the Timimoun Park's photovoltaic power distribution within the grid, two methodologies were employed: the Fast Decoupled Load Flow (FDLF) method and the Particle Swarm Optimization (PSO) technique for Optimal Power Flow (OPF).

3.1. Frequency grid evolution

At the integration point of Timimoun (bus 4), Figure 9 illustrates the progression of the synchronism frequency correction (f_r) as it relates to the frequency prediction (f_p) model.

In accordance with the forecasts generated by the f_p model, the graph depicts the variations that occur in the f_{OPF} value throughout the course of time. The f_{OPF} is a representation of the frequency correction that is desired and necessary in order to keep optimal synchronism throughout the integration point.

The proper value for the f_{OPF} is determined by the model through a comparison of the predicted frequency (f_p) with the actual frequency. This is done in order to guarantee synchronisation and stability within the system.

The success of the frequency prediction model in properly forecasting the necessary correction to preserve optimal synchronism at the integration point of Timimoun is illustrated by this graph, which provides interesting insights into the effectiveness of the model.

It assists system planners and operators in making well-informed decisions and modifications, which helps to ensure that the electrical grid continues to function in a dependable and stable manner.

The correction that was accomplished utilising the AGC at the injection bus of Timimoun is depicted in Figure 9, after which the error frequency correction is shown in Figure 10.

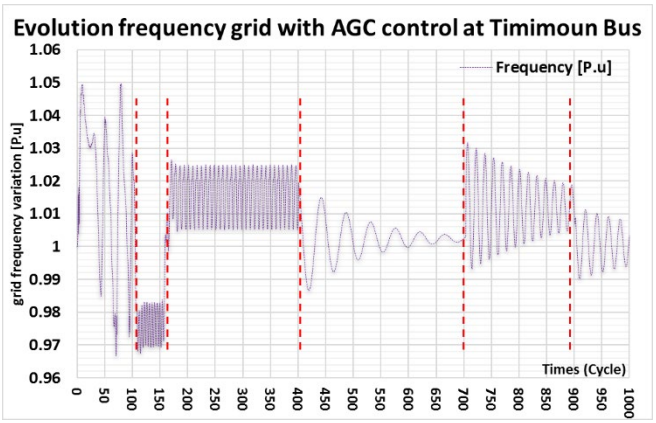

Figure 9. Frequency grid with AGC correction at Timimoun injection bus

The graph illustrates how the AGC system adjusts and regulates the power active generation of the gas turbines in response to changes in frequency fluctuations. This correction mechanism ensures that the power generation from these gas turbines aligns with the required frequency and maintains the stability of the electrical grid at the integration Timimoun bus.

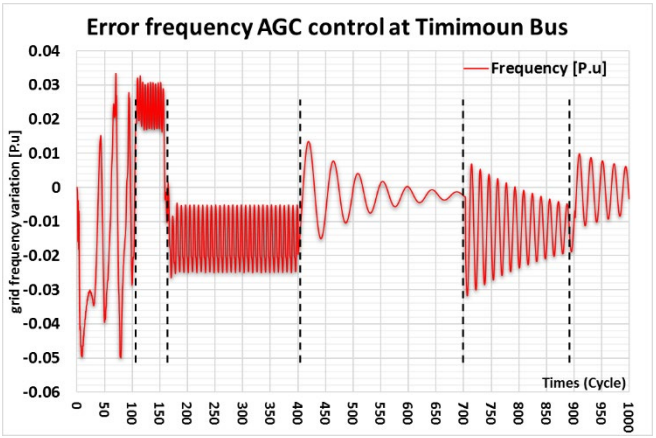

Figure 10. Frequency grid with AGC correction at Timimoun injection bus

Figure 11 illustrates the maximum voltage levels recorded at the 220 kV transmission and 30 kV distribution buses, comparing scenarios with and without the integration of PV sources under frequency control measures.

The graph highlights the peak voltages encountered during the operation of the electrical system, providing insight into the system's voltage stability.

Frequency control mechanisms, including automatic voltage regulation and reactive power compensation, are employed to ensure that voltage levels remain within acceptable limits.

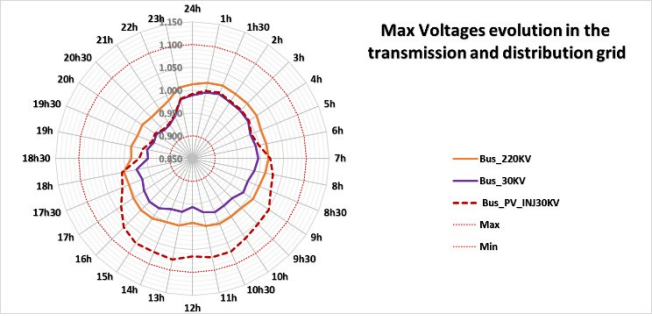

Figure 11. Evolution of Maximum Voltages in the 220 kV Transmission and 30 kV Distribution Buses with PV Integration at the Timimoun Injection Bus.

3.2. Generator productions

Figure 12 illustrates the dynamic variations in the maximum aggregate active power generation (in MW) over a 24-hour period on May 21, 2023. This includes contributions from both the gas turbines and the Timimoun photovoltaic (PV) park, with an emphasis on maintaining an optimal power factor configuration.

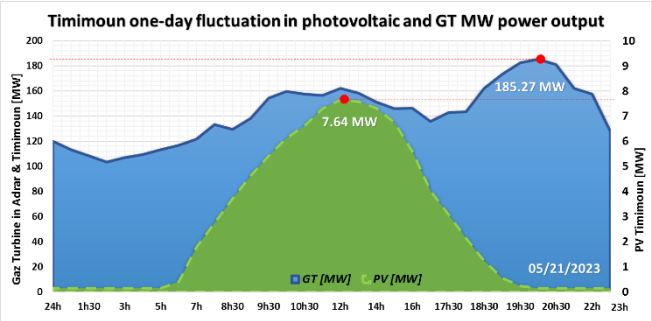

Figure 12. Active Power Generation from Gas Turbines in Adrar and Timimoun PV Park.

The Power Factor optimised to maximise power efficiency and reduce losses. The graph shows how appropriate power factor settings affect overall active and reactive power production, especially when VRE sources are integrated.

Figure 13 shows the fluctuations and interrelationships between PV injection power factor and grid (load) power factor with power factor control throughout the cycle. This diagram shows the system's power factor performance, helping operators and planners optimise power factor and manage electrical energy. The Timimoun PV Park and other energy sources affect the system power factor, which is the average power factor across the electrical grid.

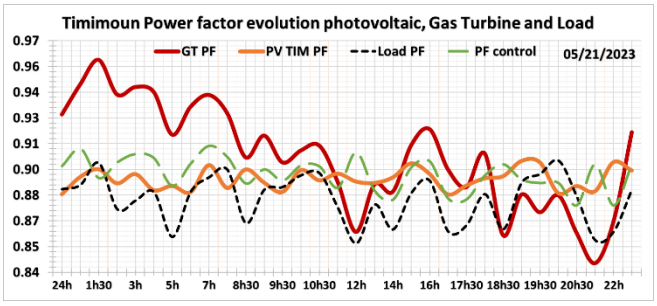

Figure 13. Global Power Factor Control per Cycle.

3.3. Active losses of the system

Figure 14 presents the results of the total active losses in the system with and without PV integration.

The graph illustrates the total active losses experienced in the electrical system under two different scenarios. The first scenario represents the total active losses without the integration of VRE, while the second scenario includes the presence of VRE in the system PF control.

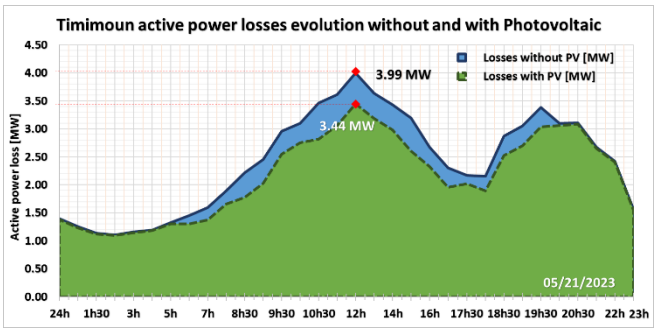

Figure 14. PIAT Total active losses in different scenario

Table 2 presents a comparison between different scenarios or interventions aimed at reducing active losses in the system. It shows the percentage by which active losses are reduced in each case, indicating the effectiveness of the respective measures or conditions.

Table 2. Reduction in percentage of max active losses

Study ID	Without VRE	With VRE
Max Loss-MW	3.998	3.443
Reduction %		**13.88**

The percentage reduction in active losses offers critical insights into the effects of integrating renewable energy sources, such as photovoltaic (PV) systems, and implementing optimization strategies on overall system efficiency. When PV systems are added to the power grid, various factors can influence megawatt (MW) losses.

Transmission and distribution losses arise due to resistance in power lines and transformers, which are affected by the location and capacity of PV installations, as well as the

distance between generation sources and load centers. Grid integration challenges, including voltage fluctuations and stability concerns, often require additional infrastructure, which can increase MW losses. The inherent variability of PV generation, due to factors like cloud cover and shading, can cause fluctuations in power output, leading to supply-demand imbalances and higher MW losses.

Effective system design and operation, including proper sizing, optimal panel positioning, and efficient inverters, are crucial in mitigating these losses. Additionally, the conversion efficiency of PV systems plays a significant role; lower efficiency leads to more energy not being converted into electricity, resulting in greater MW losses.

Despite these challenges, the environmental and sustainability benefits of solar energy often outweigh the losses, with ongoing efforts to improve PV efficiency, grid integration, and system design to minimize MW losses and maximize the advantages of PV integration.

4. Conclusion

This study underscores the critical importance of efficiently managing the integration of solar energy from the 9 MW Timimoun Photovoltaic Park in Algeria. It offers a practical solution for ensuring grid stability, reliability, and power quality while promoting the sustainable use of renewable resources. The integration of photovoltaic energy, despite its potential benefits, poses technical challenges due to dynamic power consumption patterns and meteorological variations, which can lead to frequency fluctuations and transient stability issues.

To address these challenges, we proposed an approach that combines Automatic Generation Control (AGC) with the Particle Swarm Optimization (PSO) algorithm. This method provides real-time regulation to mitigate frequency deviations caused by imbalances between production and consumption, while also optimizing the injection power factor. The effectiveness of this approach is evident in our simulations and case studies, which demonstrate significant benefits, including stabilized frequency at the Timimoun integration point and reduced total active losses within the PIAT network.

Additionally, strategic power factor control at injection buses enhances electrical power quality and maximizes the photovoltaic park's output. The results also indicate a notable reduction in natural gas consumption for the gas turbines in Adrar and Timimoun, with a 4.84% decrease in overall production for the PIAT network on May 21, 2023, attributed to the Timimoun park's 86.82 MW output over 24 hours.

The findings of this study are highly relevant to the Algerian Electric System Operator (AESO) and researchers focused on renewable energy and sustainable electrification. By adopting the proposed approach, the integration of renewable energy sources can be optimized, leading to improved grid stability, economic advantages, and a reduced carbon footprint, thereby contributing to a greener and more sustainable energy future for Algeria.

Appendix A.

Table 3 presents parameters of the control system:

Table 3. Parameters of the Control System

Parameters	value
Turbine Pulse Frequency $\boldsymbol{\omega_T}$	$\mathbf{2\ rad/s}$
Governor Pulse Frequency $\boldsymbol{\omega_g}$	$\mathbf{5\ rad/s}$
System Pulse Frequency $\overrightarrow{\boldsymbol{\omega_{Tg}}}$	$\mathbf{10\ rad/s}$
Generator inertia constant $\boldsymbol{H}$	$\mathbf{5\ s}$
Governor speed regulation $\boldsymbol{R_g}$	$\mathbf{0.05\ P.u}$
Load variation $\Delta \boldsymbol{P_L}$	$\mathbf{0.376\ P.u}$
Steady-state frequency deviation $\Delta\boldsymbol{\omega}$	$\mathbf{-0.0182\ P.u}$

References

[1] A. A. Tadjeddine, M. S. Bendelhoum, R. I. Bendjillali, H. Hamiani, and S. Djelaila, "VRE integrating in PIAT grid with AFRR using PSS, MPPT, and PSO-based techniques: A case study kabertene," EAI Endorsed Transactions on Energy Web, vol. 10, 2023. doi:10.4108/ew.3378

[2] T. A. Abderrazak et al., "Enhancing frequency system damping efficiency via optimal integration of VRE in grid," 2023 Second International Conference on Energy Transition and Security (ICETS), pp. 1–6, Dec. 2023. doi:10.1109/icets60996.2023.10410747

[3] A. Bouraiou et al., "Temperature supervision and monitoring based on embedded controller using SCADA platform," 2024 2nd International Conference on Electrical Engineering and Automatic Control (ICEEAC), pp. 1–5, May 2024. doi:10.1109/iceeac61226.2024.10576405

[4] A. Lagouch, R. Maouedj, A. Benatiallah, S. Regragui, and M. Benhadji, "20 MW solar power plant performance analysis under Saharan condition," 2024 2nd International Conference on Electrical Engineering and Automatic Control (ICEEAC), pp. 1–5, May 2024. doi:10.1109/iceeac61226.2024.10576275

[5] F. Osorio, M. A. Mantilla, J. M. Rey, and J. F. Petit, "A flexible control strategy for multi-functional PV inverters with load compensation capabilities considering current limitations and unbalanced load conditions," Energies, vol. 17, no. 17, p. 4218, Aug. 2024. doi:10.3390/en17174218

[6] S. M. S. Ullah, S. Ebrahimi, F. Ferdowsi, and M. Barati, "Techno-economic impacts of volt-var control on the high penetration of solar PV interconnection," Cleaner Energy Systems, vol. 5, p. 100067, 2023. doi:10.1016/j.cles.2023.100067

[7] A. Guenounou, M. Aillerie, and D. Lafri, "Modeling of the household electricity consumption in the regions of southern Algeria. Proposition of a new subsidy plan," technologies and materials for renewable energy, environment and sustainability: TMREES22Fr, 2023. doi:10.1063/5.0129394.

[8] A. Hilawie and F. Shewarega, "Static Voltage Stability Assessment of Ethiopian power System Using Normalized Active Power Margin Index", EAI Endorsed Trans Energy Web, vol. 9, no. 40, p. e5, Dec. 2022.

[9] N. Rajesh, M. Venu Gopala Rao, and R. Srinivasa Rao, "Power Quality Improvement using Parallel Connected FACTS Device with Simplified d-q Control", EAI Endorsed Trans Energy Web, vol. 9, no. 40, p. e2, Jul. 2022.
[10] H. Dehghani Tafti et al., "Adaptive Power System frequency support from distributed photovoltaic systems," Solar Energy, vol. 257, pp. 231–239, 2023. doi:10.1016/j.solener.2023.04.017.
[11] D. E. Abah, G. S. Shehu, A. S. Abubakar, and S. Salisu, A novel multistage controller for load frequency control of a multi-area network integrated with Renewable Energy Sources, Oct. 2023. doi:10.21203/rs.3.rs-3385334/v1
[12] A. M. Ewais et al., "Adaptive frequency control in smart microgrid using controlled loads supported by real-time implementation," PLOS 1, vol. 18, no. 4, 2023. doi:10.1371/journal.pone.0283561
[13] P. Fan et al., "A Load Frequency coordinated control strategy for multimicrogrids with V2G based on improved Ma-DDPG," International Journal of Electrical Power & Energy Systems, vol. 146, p. 108765, 2023. doi:10.1016/j.ijepes.2022.108765
[14] G. M. Meseret and L. C. Saikia, "AGC in the multi-area thermal system with integration of distribution generation on the frequency of the system using the classical PID & Hybrid Neuro-Fuzzy Controllers," IETE Journal of Research, pp. 1–10, 2022. doi:10.1080/03772063.2022.2083024
[15] T. Lei et al., "Performance analysis of grid-connected distributed generation system integrating a hybrid wind-PV farm using UPQC," Complexity, vol. 2022, pp. 1–14, 2022. doi:10.1155/2022/4572145.
[16] D. K. Mishra, L. Li, J. Zhang, and Md. J. Hossain, "Challenges and viewpoints of load frequency control in deregulated power system," Power System Frequency Control, pp. 117–132, 2023. doi:10.1016/b978-0-443-18426-0.00010-8
[17] A. Gupta, "Power Quality Evaluation of photovoltaic grid interfaced cascaded H-bridge nine-level multilevel inverter systems using D-STATCOM and UPQC," Energy, vol. 238, p. 121707, 2022. doi:10.1016/j.energy.2021.121707
[18] M. Zolfaghari and G. B. Gharehpetian, "Decentralized Power Exchange control methods among subsystems in future power network," Decentralized Frameworks for Future Power Systems, pp. 345–367, 2022. doi:10.1016/b978-0-323-91698-1.00003-0
[19] P. Kuntal, A. Mathur, and M. N. Alam, "Optimal Power Scheduling of Hybrid Power System," 2021 IEEE 2nd International Conference on Smart Technologies for Power, Energy and Control (STPEC), 2021. doi:10.1109/stpec52385.2021.9718620.
[20] J. N. Namratha, P. Venkatasubramanian, and A. Rama Koteswara Rao, "A hybrid SCSO-QNN approach based load frequency control of three area power system with renewable sources using FOPID controller," Smart Science, pp. 1–15, Jun. 2024. doi:10.1080/23080477.2024.2355747
[21] S. Kim, "A novel preventive frequency stability constrained OPF considering wind power fluctuation," 2022 IEEE PES Innovative Smart Grid Technologies - Asia (ISGT Asia), 2022. doi:10.1109/isgtasia54193.2022.10003619
[22] A. A. Tadjeddine, M. S. Bendelhoum, I. Arbaoui, R. I. Bendjillali, and M. Alami, "Optimizing Frequency Stability in Distributed Power Grids through Advanced Power Flow Control with 25MW Photovoltaic Integration", Adv Syst Sci Appl, vol. 23, no. 4, pp. 18–30, Dec. 2023.
[23] S. Shukla, A. Gupta, and R. Pandey, "Load frequency control for multi-area power system using PSO-based technique," Artificial Intelligence Techniques in Power Systems Operations and Analysis, pp. 17–35, 2023. doi:10.1201/9781003301820-2
[24] B. Khokhar, K. P. Parmar, T. Thakur, and D. P. Kothari, "LFC Study of a multi-microgrid system," Load Frequency Control of Microgrids, pp. 133–145, May 2024. doi:10.1201/9781003477136-9
[25] T. A. Abderrazak, A. Iliace, H. Hichem, B. Mohamed Sofiane, and B. Ridha Ilyas, "Robust hybrid control strategy for active power management in Kabertene wind farm within Algeria's Piat Grid," Bulletin of Electrical Engineering and Informatics, vol. 13, no. 4, pp. 2202–2212, Aug. 2024. doi:10.11591/eei.v13i4.7270
[26] K. WADHWA and S. K. Gupta, "Cuckoo search optimization technique for automatic generation control (AGC) in an integrated power system with multiple power sources," 2023. doi:10.2139/ssrn.4401463
[27] M. Berto, L. Alberti, and S. Bolognani, "Measurement of the self-sensing capability of synchronous machines for high frequency signal injection sensorless drives," IEEE Transactions on Industry Applications, vol. 59, no. 3, pp. 3381–3389, 2023. doi:10.1109/tia.2023.3241887
[28] D. Li, W. Hua, and Y. Mi, Estimation of power system inertia constant using bayesian inertia estimation method, 2024. doi:10.2139/ssrn.4747552
[29] H. Abubakr et al., "Adaptive LFC incorporating modified virtual rotor to regulate frequency and tie-line power flow in multi-area microgrids," IEEE Access, vol. 10, pp. 33248–33268, 2022. doi:10.1109/access.2022.3161505
[30] R. W. Kenyon et al., "Autonomous Grid-Forming Inverter Exponential Droop Control for Improved Frequency Stability," pp. 1–10, 2024. doi: 10.48550/arXiv.2408.12709
[31] X. Chen, Y. Jiang, V. Terzija, and C. Lu, "Review on measurement-based frequency dynamics monitoring and analyzing in renewable energy dominated Power Systems," International Journal of Electrical Power & Energy Systems, vol. 155, p. 109520, Jan. 2024. doi:10.1016/j.ijepes.2023.109520
[32] M. Muftić Dedović, S. Avdaković, M. Musić, and I. Kuzle, "Enhancing power system stability with adaptive under frequency load shedding using SYNCHROPHASOR measurements and empirical mode decomposition," International Journal of Electrical Power & Energy Systems, vol. 160, p. 110133, Sep. 2024. doi:10.1016/j.ijepes.2024.110133
[33] L. Meegahapola, S. Bu, and M. Gu, "Frequency stability and control of hybrid AC/DC power grids," Power Systems, pp. 161–188, 2022. doi:10.1007/978-3-031-06384-8_6
[34] A. K. Mohapatra, S. Mohapatra, A. Pattnaik, and P. C. Sahu, "Design and modelling of an AI governed type-2 fuzzy tilt control strategy for AGC of a multi-source power grid in constraint to optimal dispatch," e-Prime - Advances in Electrical Engineering, Electronics and Energy, vol. 7, p. 100487, Mar. 2024. doi:10.1016/j.prime.2024.100487
[35] Z. Wang, Y. Wang, Z. Ding, J. Wu, and K. Zhang, "Optimal AGC allocation strategy based on data-driven forecast of frequency distribution key parameters,"

Electric Power Systems Research, vol. 226, p. 109916, Jan. 2024. doi:10.1016/j.epsr.2023.109916

[36] P. Zhao, Z. Li, X. Bai, J. Su, and X. Chang, "Stochastic real-time dispatch considering AGC and electric-gas dynamic interaction: Fine-grained modeling and noniterative decentralized solutions," Applied Energy, vol. 375, p. 123976, Dec. 2024. doi:10.1016/j.apenergy.2024.123976

[37] P. Maucher, S. Remppis, D. Schlipf, and H. Lens, "Handling limitations in the Interzonal exchange of Automatic Frequency Restoration Reserves," IFAC-PapersOnLine, vol. 56, no. 2, pp. 1437–1442, 2023. doi:10.1016/j.ifacol.2023.10.1823

[38] D. Cremoncini et al., "Optimal participation of a wind and hybrid battery storage system in the day-ahead and Automatic Frequency Restoration Reserve Markets," Journal of Energy Storage, vol. 94, p. 112309, Jul. 2024. doi:10.1016/j.est.2024.112309

[39] W. Kang et al., "Distributed control of virtual energy storage systems for voltage regulation in low voltage distribution networks subjects to varying time delays," Applied Energy, vol. 376, p. 124295, Dec. 2024. doi:10.1016/j.apenergy.2024.124295

[40] L. Deman and Q. Boucher, "Impact of renewable energy generation on Power Reserve Energy Demand," Energy Economics, vol. 128, p. 107173, Dec. 2023. doi:10.1016/j.eneco.2023.107173